Astron. Astrophys. 316, 464–480 (1996)

ASTRONOMY
AND
ASTROPHYSICS

The high latitude pass of ULYSSES: energetic particle observations with EPAC

E. Keppler[1], **B. Drolias**[2], **M. Fraenz**[3], **A. Korth**[1], **M.K. Reuss**[1], **B. Blake**[4], **and J.J. Quenby**[2]

[1] Max-Planck-Institut für Aeronomie, Postfach 20, D-37189 Katlenburg-Lindau, Germany
[2] Imperial College of Science and Technology, The Blackett Laboratory, Prince Consort Road, London SW7 2BZ, England
[3] Astronomy Unit, Queen Mary & Westfield College, Mile End Road, London E1 4NS, England
[4] Aerospace Corporation, Space Sciences Laboratory, POB 92957, Los Angeles, CA 90009-2957, USA

Received 16 February 1996 / Accepted 20 June 1996

Abstract. We report on observations of energetic particles (EP) during the ascent of ULYSSES to the south pole, on the fast pass from south to north and in the first few months after the north polar pass. After it left the ecliptic plane the spacecraft moved periodically into a corotating (26 days period) fast solar wind stream and observed the accelerated EP associated with the forward and reverse shocks. Such particles were observed up to 68° in heliographic latitude. Only when ULYSSES returned to lower latitudes did the accelerated beams reappear. The fast pass from south to north polar regions showed on a compressed timescale similar features to those already observed on the ascending part. Apparently the recurrence period of the EP did not change throughout that pass. No evidence for differential rotation could be found in our data. The north polar pass again did not show energetic particles to be present at such high latitudes. In regions where the intensities were low, we identified from the C/O ratio and oxygen spectrum an underlying population of anomalous cosmic rays (ACR), which show a bidirectional field aligned anisotropy. The appearance of the EPs was anticorrelated to the modulated ACR and GCR fluxes. We conclude that ACR and GCR were modulated by the corotating interaction regions (CIR); shocks associated with them accelerated the observed EP streams. During the fast polar pass the latitudinal gradient of GCR protons was determined to be 0.3 to 0.4%/degree.

Key words: cosmic rays – shock – acceleration of particles – interplanetary medium

Send offprint requests to: E. Keppler

1. Instrument description

The EPAC instrument consists of four identical three element semiconductor telescopes mounted at different angles relative to the spacecraft spin axis so that by virtue of the spin rotation about 80% of the sphere is sampled in 32 bins. By means of the (dE/dx)-E technique elements up to iron can be separated. The energy ranges covered are 0.3 to 1.5 MeV for protons, and 0.4 to 6 MeV/N for heavier ions. Electrons are measured in two channels (0.1<E<0.38 MeV,"ELL", and E>0.18 MeV, "ELH"), spin averaged for each telescope. The ELH channels are also sensitive to RTG gammas (in the MeV range) and to high energy protons, which may penetrate the 1.5 mm Pt shield (dependent on direction: E>230 MeV), so both contribute to the observed background counts. Electrons of higher energies are typically transient events. In times between their appearance the rates often drop to background levels. After launch RTG gammas and GCR proton contributions rose with time, the gammas because of the decay processes in the RTG, the protons because of the increase of their flux in the declining solar cycle. The minimum rates in these channels, from launch to day 100/1992, were found to increase almost exponentially with time constants T_o = 21 years. In order to use the ELH data as a record of the GCR protons in the absence of electrons a comparison was made with a channel of the COSPIN-KET telescope on ULYSSES of similar energies (courtesy H. Kunow). This allowed us to isolate the RTG background which was then extrapolated with the time constant mentioned and subtracted from the ELH rates. Due to the telescopes' different orientation relative to the RTG the corrections are slightly different for the four telescopes (between 1 and 1.8 counts/s), while the rates due to protons range from 0.5 to 0.7 c/s (after day 100/1992). These corrected rates were found to follow the COSPIN-KET channel closely (cf. Simpson et al. 1995).

A detailed description of the instrument can be found in Keppler et al. (1992).

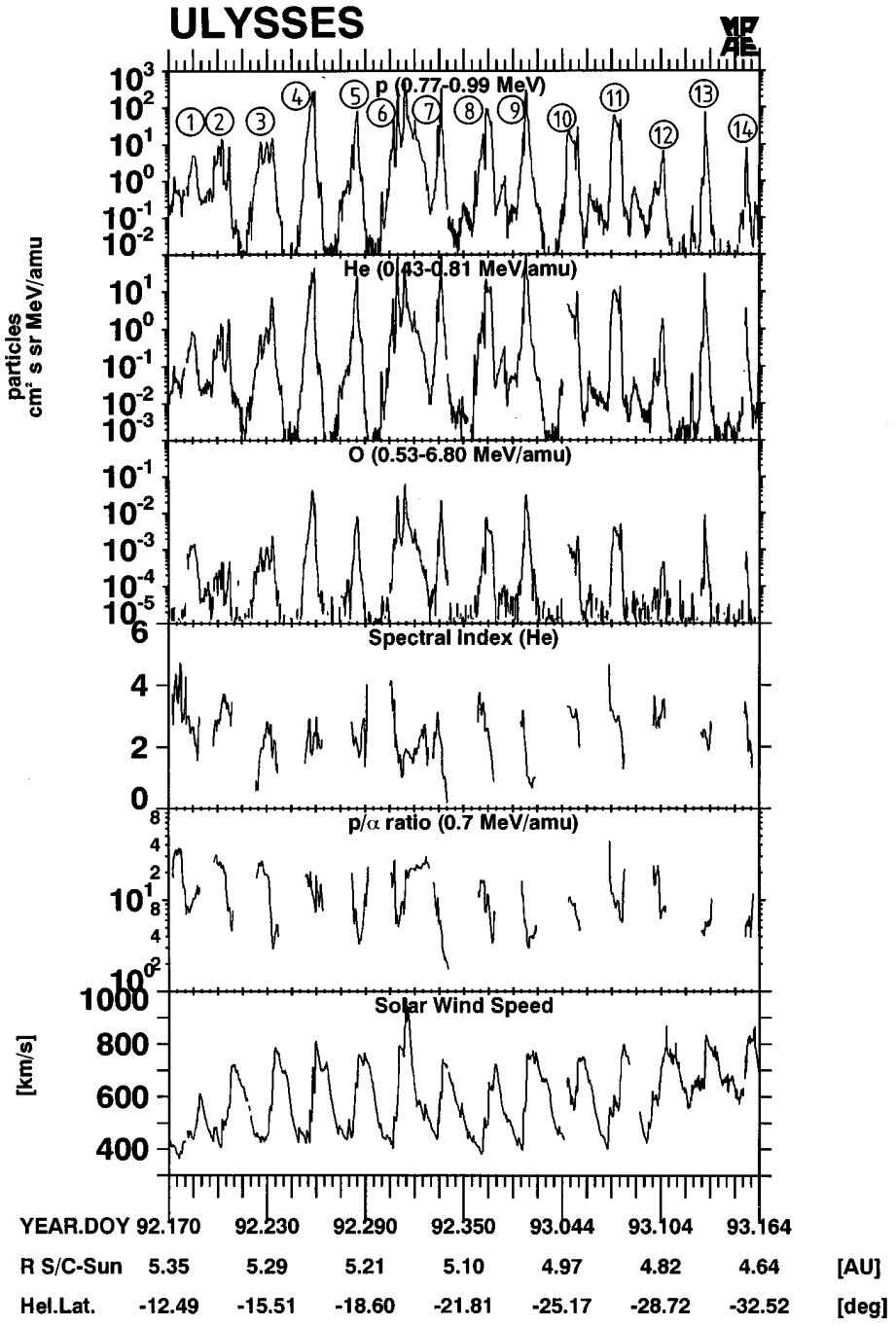

Fig. 1a. From top: Fluxes of energetic protons, helium and oxygen (energy ranges given in figure), spectral index for He (assuming power law in E/N), p/He ratio at 0.7 MeV/N and solar wind speed, taken from SWICS (courtesy G. Gloeckler) from day 170/1992 until day 164/1993, while ULYSSES passed from 12° to 32° S latitude. Peaks of CIR associated accelerated particle beams are identified by numbers.

2. The CIR-Encounters

2.1. Observations

When ULYSSES left the ecliptic plane after its Jupiter swingby, it encountered a region dominated by fast solar wind which originated in the equatorward extension of the southern polar coronal hole. Its velocities reached almost 800 km/s, while outside of that region the solar wind speed dropped to about 400 km/s (Bame et al. 1993). When a fast solar wind stream rams into slow wind ahead of it, beyond 1 AU a corotating interaction region (CIR) will be formed, typically bounded by a forward (F)/reverse (R) shock pair (Hundhausen & Gosling 1976, Smith & Wolfe 1976). This situation was also experienced by ULYSSES (Balogh et al. 1993, Smith et al. 1993).

During each of the 19 encounters with the CIR, the EPAC instrument on ULYSSES observed an increase in the EP fluxes. These increases reappeared in 26.6 days intervals due to the corotation of the fast solar wind streams with the Sun. The particles have apparently been accelerated by the F- and R-shocks associated with the CIR. These kind of observations are of course not new and in fact have been made earlier (see, e.g., Barnes & Simpson 1976); however, in the case of ULYSSES the number

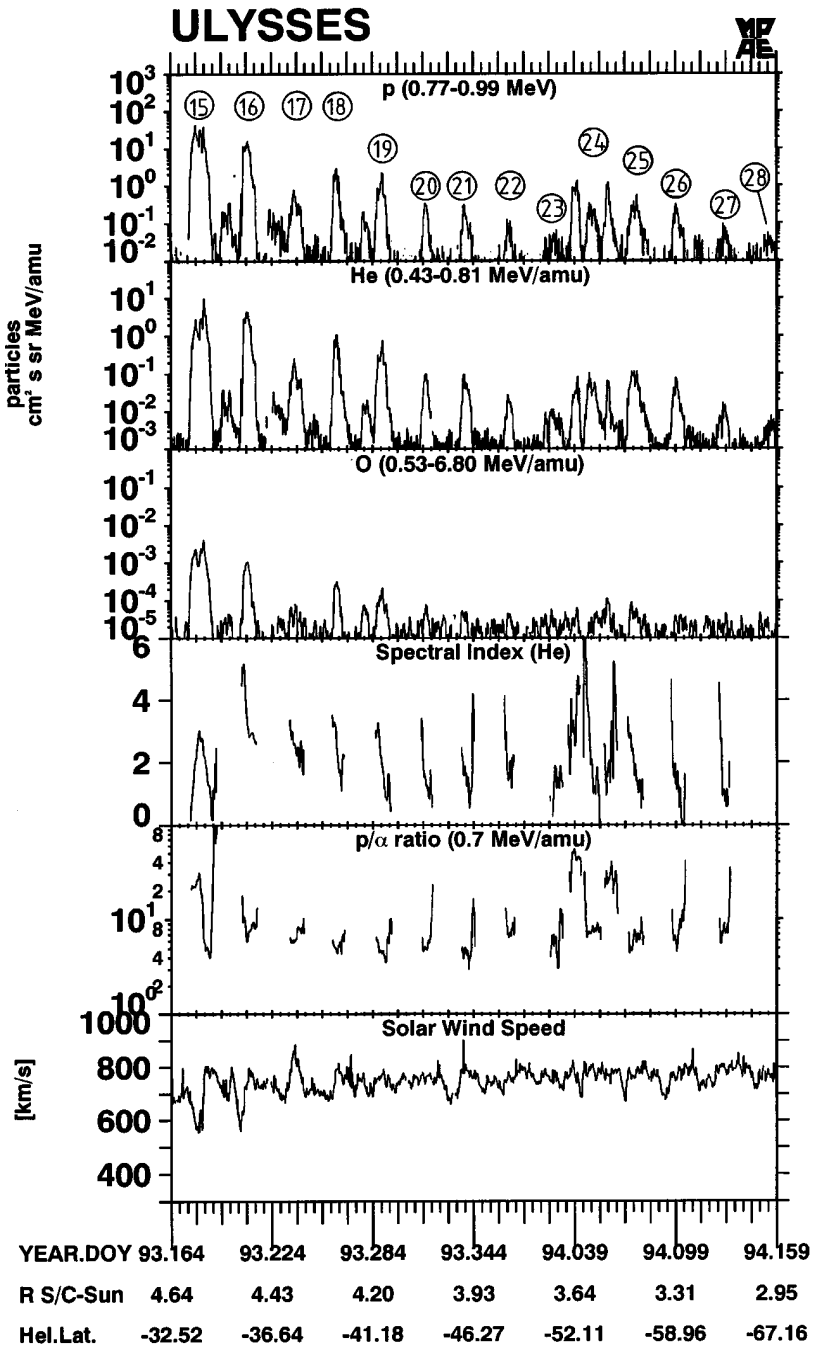

Fig. 1b. Same as Fig. 1a, but for 164/1993 to 159/1994, while ULYSSES passed from 32° to 67°S latitude.

of such events will allow for a more thorough study which is presently being prepared. Therefore we will restrict ourselves in this summary paper to the most characteristic aspects of these events.

Figs. 1a and 1b give an overview of EPAC observations of protons, helium and oxygen together with the solar wind speed (derived from SWICS data, courtesy G. Gloeckler). We have added numbers to the observed corotating particle fluxes for reference. The figures show that the intensity in the energetic particle channels begins to rise well ahead of the approaching fast solar wind stream. In Table 1 we have summarized various characteristic features which can be obtained for the various streams. We note that in some cases "secondary" peaks can be seen between the accelerated particle peaks. These have been termed "interevents" by Roelof et al. (1994); they are not related to the CIRs but are of rather solar origin.

It can be seen in Figs. 1a and 1b that associated with the passage of the forward/reverse shock pairs ahead of/behind the CIR interface the particle fluxes rose in some cases by more than four orders of magnitude in all species. We tentatively assume that these particles have been accelerated by the shocks that accompany the CIR. The shocks were identified according to Balogh et al. (1995). Such a pattern was seen throughout 1992 to mid 1993. Typical features of accelerated particles known for

Table 1. Characteristic features of the events indicated in Figs. 1 by numbers.

	F-Shock Related				R-Shock Related			
#	Peak Flux[1)]	γ[3)]	p/He[6)]	e^--Rate[2)5)]	Peak Flux[1)]	γ[3)]	p/He[6)]	e^--Rate[2)]
1	0.006	3	10	–	–	–	–	–
2	0.08	3	25	–	0.15	2.5	8	–
3	0.08	2.5	25	–	0.05	2	3	35
4	15	3	20	–	40	1.8	6.5	20
5	1	2.8	35	(10)	40	2	5.5	70
6	Complex event, transients involved.							
7[7)]	7	3	11	(37)	103	1	5.5	663
8	4	3.3	18	(29)	15	2.5	3	268
9	7	3.3	30	(38)	105	1.5	8	1780
10[7)]	1.5	3	20	(38)	10	2	10	47
11[4)]	0.03	3.5	50	–	10	3	12	96
	7	3	10	(82)	15	2.2	6	83
12	–	–	–	–	2	~ 2	20	–
13	–	–	–	–	40	2	8	149
14	0.02	3.5	?	–	4.5	3	10	11
15	3	3	30	–	20	1	4	127
16	–	–	–	–	3	3	6	11
17[7)]	–	–	–	–	0.2	2.3	10	–
18	–	–	–	–	1	3	5	–
19	–	–	–	–	0.8	2	4	–
20	–	–	–	–	0.1	1	5	–
21	–	–	–	–	0.1	2	5	–
22	–	–	–	–	0.02	1.5	8	–
23	–	–	–	–	0.006	1	5	–
24	–	–	–	–	0.06	2	12	–
25	–	–	–	–	0.1	2	6	–
26	–	–	–	–	0.07	1	6	–
27	–	–	–	–	0.015	1	7	–
28	–	–	–	–	0.008	–	–	–

1) He flux for 0.4–0.8 MeV/N in particle/cm^2 s sr MeV/N.
2) Electrons in particle/cm^2 s sr MeV.
3) Exponent $-\gamma$ for a power law fit.
4) Double event.
5) Values in parenthesis: Association to shock not clear.
6) p/He ratio for 0.7 MeV/N.
7) No shock reported from plasma and magnetic field data, however, shock relation likely from particle data.

CIR related shock pairs in lower latitudes were also observed in the higher latitudes. These include a short rise in front of the F-shock (when ULYSSES was still in the slow wind domain) to a first peak in ion intensity at the F-shock surface, followed by a decay toward the stream interface. Thereafter an even larger increase in intensity of ions but also in some cases in electron flux occurs at the time when the R-shock passes by. This shock is followed by a slow EP decay when the spacecraft becomes immersed in the fast solar wind stream.

In Figs. 2a and 2b electrons ($100 < E < 380\ keV$) are shown along with the helium flux ($0.43 < E/N < 0.81\ MeV/N$) for the period 330/92 to 264/93, which is well within the region where shocks reached ULYSSES. It can be seen that the relative increase in the intensity of electrons (100–380 keV) is in general smaller than for the ions, but ions and

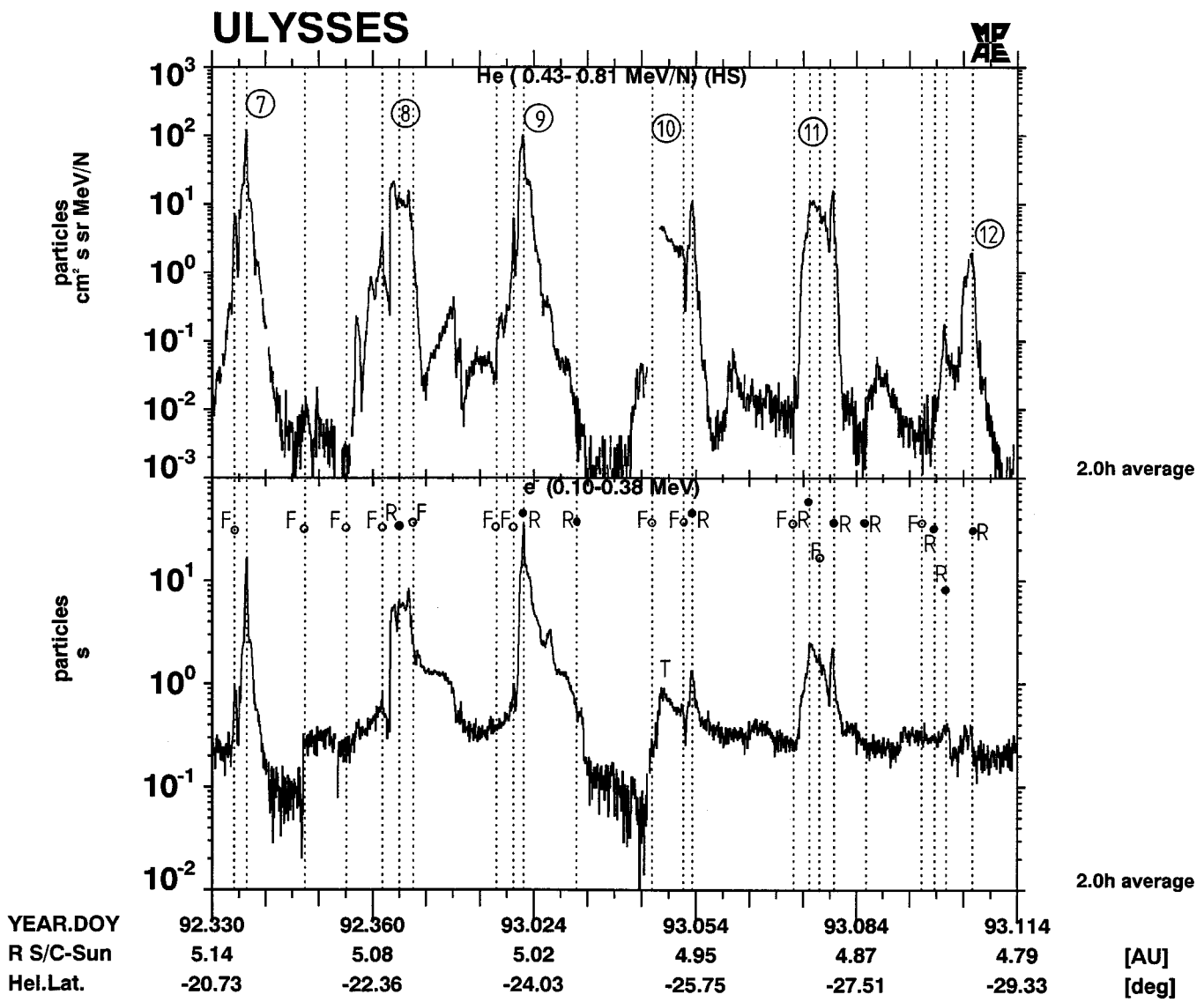

Fig. 2a. Energetic helium (0.43–0.81 MeV/N) fluxes and electron fluxes (0.1–0.38 MeV) plotted vs. time for the period 330/1992–114/1993. Dashed lines indicate observed shocks at ULYSSES (from Balogh et al. 1995). "F" or an open circle indicate forward shocks, "R" or closed circles indicate reverse shocks, "T" indicates transient events. 2 hour averages are shown. Peaks of particle fluxes are numbered, numbers correspond to those shown in Figs. 1.

electrons reach their intensity maxima by the time of the passage of the R-shock (vertical lines in Fig. 2, F: forward, R: reverse shock, both related to CIR, T: shock related to transient event). This is true for all other ion species as well. It was, however, not clear whether some weak electron fluxes observed near F-shocks were related to these shocks at all. There are, however, transient events (T), where electrons arrive simultaneously with the ions; those will not be discussed here. The last electron event (E>100 keV) associated with a CIR was observed with ion event #13 at about $-30°$ latitude, when the S/C left the streamer belt. Electrons above 100 keV finally disappeared completely above $-30°$ latitude.

Energy spectra of accelerated ions as observed within our limited energy range typically hardened in the course of such an event from near $\gamma \sim 3$ at the F-shock to about $\gamma \sim 2$ at the R-shock (if expressed as a power law in kinetic energy with $-\gamma$ as the exponent). The p/He ratio dropped typically after the passage of the F-shock from values of > 40 to < 10, sometimes to values as low as 3, which is quite unusual (see Figs. 1a and 1b). The lowest values in the p/He ratio are reached after the R-shock; it rises again with increasing distance from the shock still within the fast solar wind stream. Recently Simnett et al. (1995) attributed this change in the p/He ratio to pick-up helium, accelerated at the reverse shock.

The risetime to the intensity maxima of these ion streams did not change significantly throughout the period of observation, including the low latitude period where shocks and accelerated particles have been observed directly at ULYSSES. However,

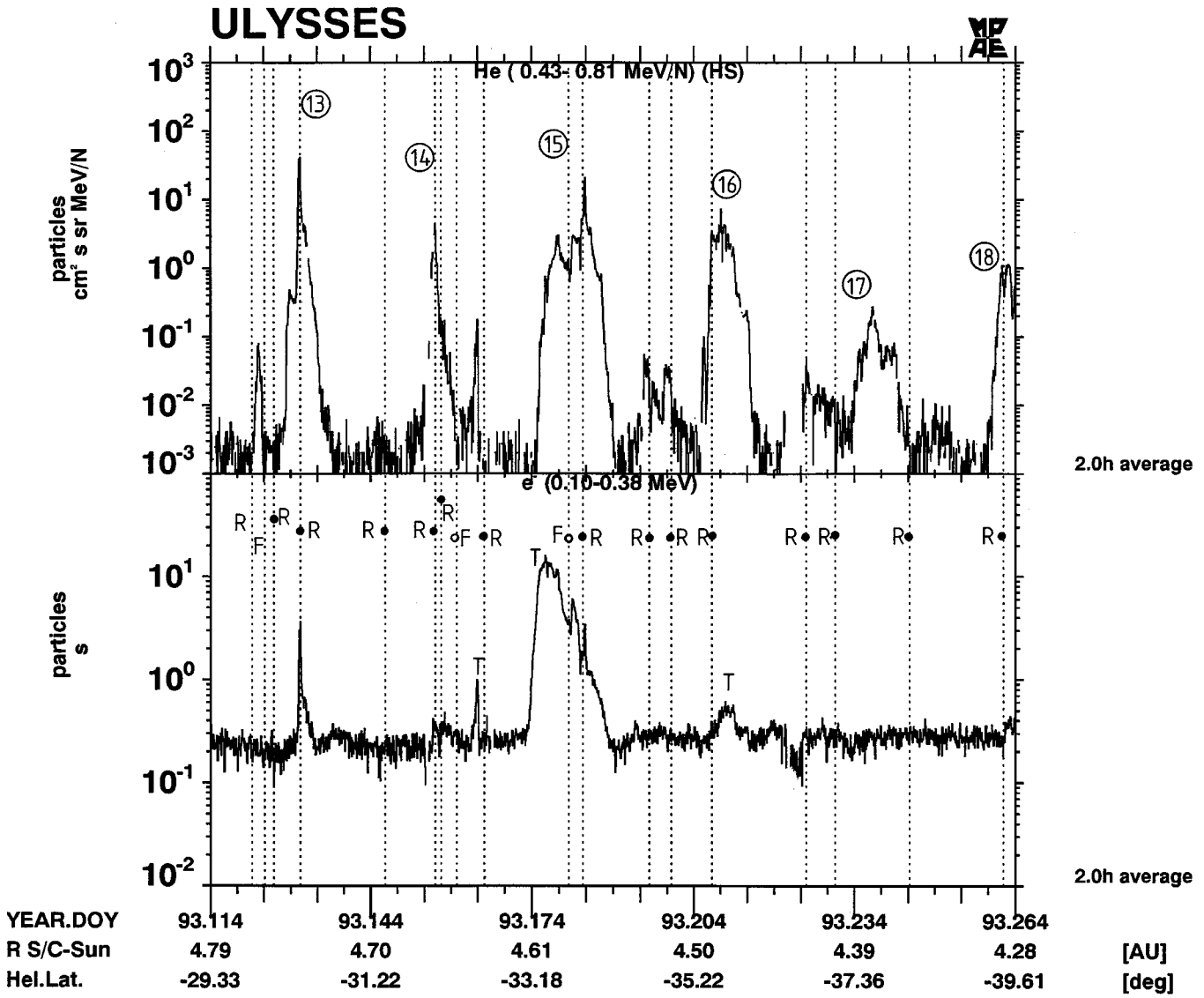

Fig. 2b. Same as Fig. 2a, but for 114/1993 to 264/1993.

these events did not show energy dispersion as illustrated for three such events in Fig. 3. This behavior seems to be typical for all events observed so far by our instrument; in those events where the counting rates were low, an upper limit of about 3 AU can be given for the distance along the average Parker spiral field which the particles of lowest and highest energies could have travelled if released at some source region at the same time. For larger distances travelled dispersion would have been noticed.

We also attempted to determine anisotropies; this, however, was difficult due to the relatively low counting rates observed in most of the events. For the present paper we restrict ourselves therefore to a few events shown in Fig. 4, where a more straightforward interpretation is possible. Here a weak but inward directed anisotropy was found (in the solar wind frame). We will publish a more extended analysis of these events in a forthcoming paper.

At higher latitudes we cannot find a correlation of the particle flux increases with variations of the solar wind speed or the interplanetary magnetic field. Both scarcely vary above 35°. However, the energetic particle fluxes continued to return in each solar rotation until June 1994, when ULYSSES had moved beyond −68°.

Subject to the fact that the back detectors of EPAC were switched off during the periods indicated in Sect. 6.1, the reappearance of energetic particle streams as observed by EPAC during the fast pass from south to north heliographic latitudes shown in Fig. 5 was observed only when ULYSSES had reached about −43° on day 365/1994. This agrees quite well with other observations for the reappearance of the corotating particle streams (e.g. Sanderson et al. 1995). This latitude was substantially lower compared to that found in the ascent to high southern latitudes. Near −18° on day 40/1995, ULYSSES again passed through the slow solar wind region until day 86/1995 at about

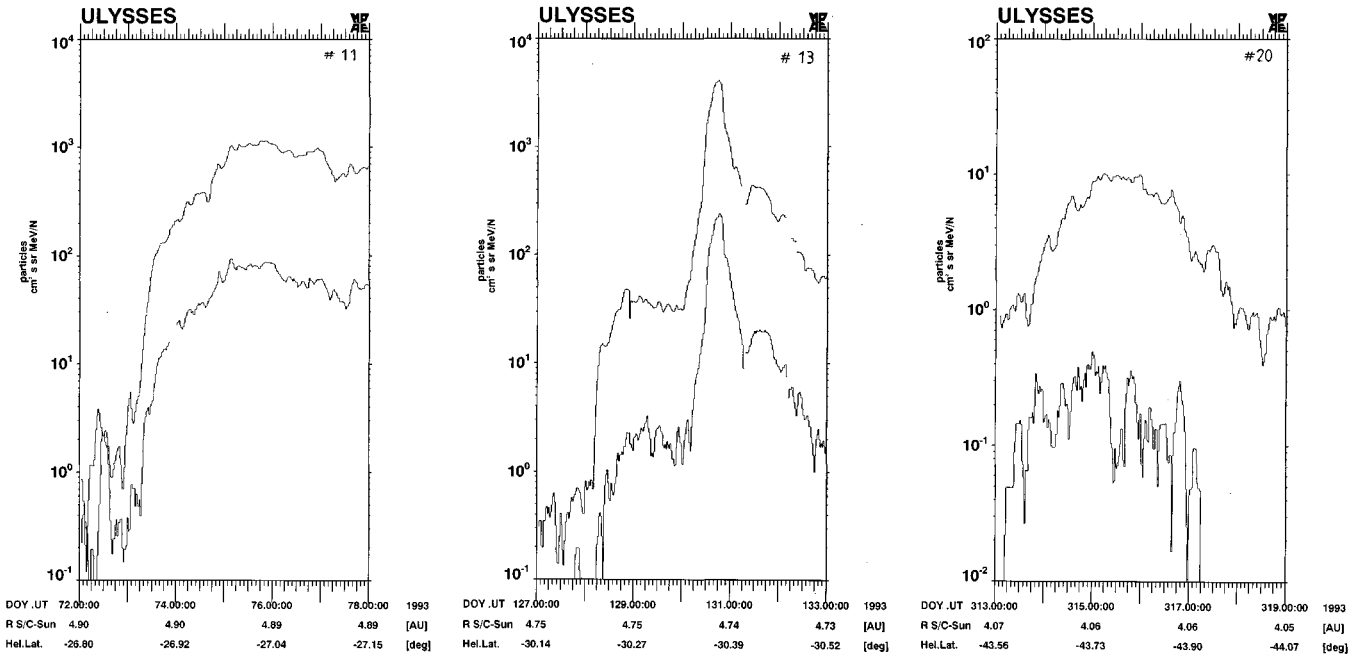

Fig. 3. Energy dispersion for 3 CIR events are shown for two He energy channels: $0.43 < E/N < 0.81$ MeV/N (v=9100-12500 km/s) and $0.2 < E < 0.29$ MeV/N (v=6200 − 7500 km/s) for the events # 11, 13, 20 (see Figs. 1 for the numbers).

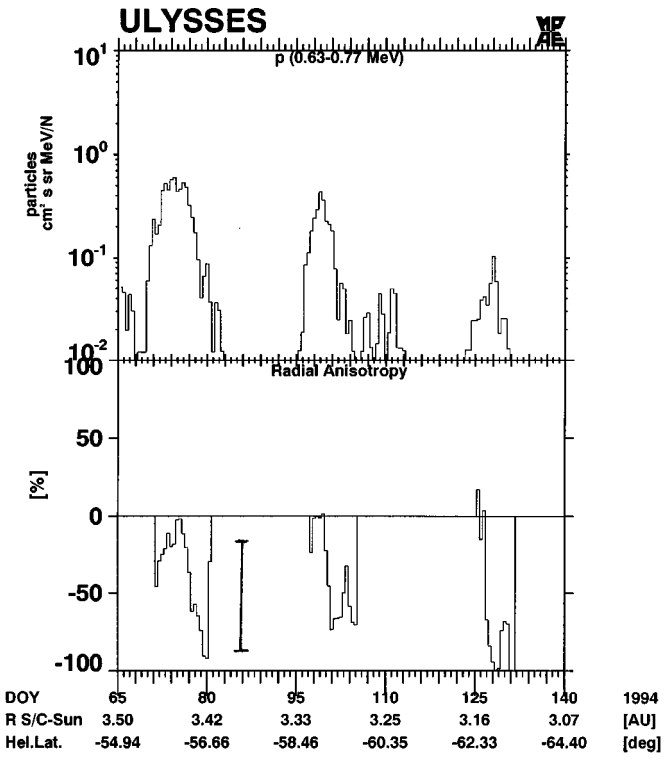

Fig. 4. The radial component R of the first order radial anisotropy in the solar wind frame (RTN coordinate system) is shown (in %, lower panel) together with the fluxes of protons (0.63–0.77 MeV) of three events (number 25, 26, and 27 from Figs. 1). Negative values of R of indicate particle streaming towards the Sun. Error bars are indicated: statistical error plus error due to fit procedures, in the lower panel.

19° north latitude (Phillips et al. 1995), when solar particle fluxes associated with solar active regions were observed. Here solar electrons were also recorded. Again this latitude was lower than the latitude on the ascending part of the orbit, where the streamer belt was left near −30°. This is probably due to the further reduction of the tilt angle of the heliomagnetic current sheet towards its solar minimum configuration (e.g. Hoeksema 1995). In the equatorial region the peaks appeared in about 13 day intervals, suggesting a 4 sector structure of the heliospheric magnetic field. Such recurrent fluxes were no longer observed after day 111/95 (see Fig. 5), which corresponds to +36° latitude. During the north polar pass again only weak particle fluxes have been observed.

2.2. Discussion

At the F-shocks the intensity of ions increased in some cases from near background levels (the observed background level for He is 10^{-4} (cm^2 sr s MeV/N)$^{-1}$). In other cases the intensity was already somewhat enhanced due to a preceding event so that the relative flux increase became smaller. The apparent time coincidence of particles and shocks suggests that the particles have been accelerated at the shocks. A background of particles of several tens of keV was always present as observed by the HI-SCALE instrument (E. Roelof, private communication, 1996); these particles could have been the seed particles from where acceleration started. On the other hand Gloeckler et al. (1994) suggested that pick-up ions (H and He) had been accelerated by shocks in the interplanetary medium to MeV energies. To interpret this as a consequence of a general energization process seems to be straightforward, even if the time constants involved

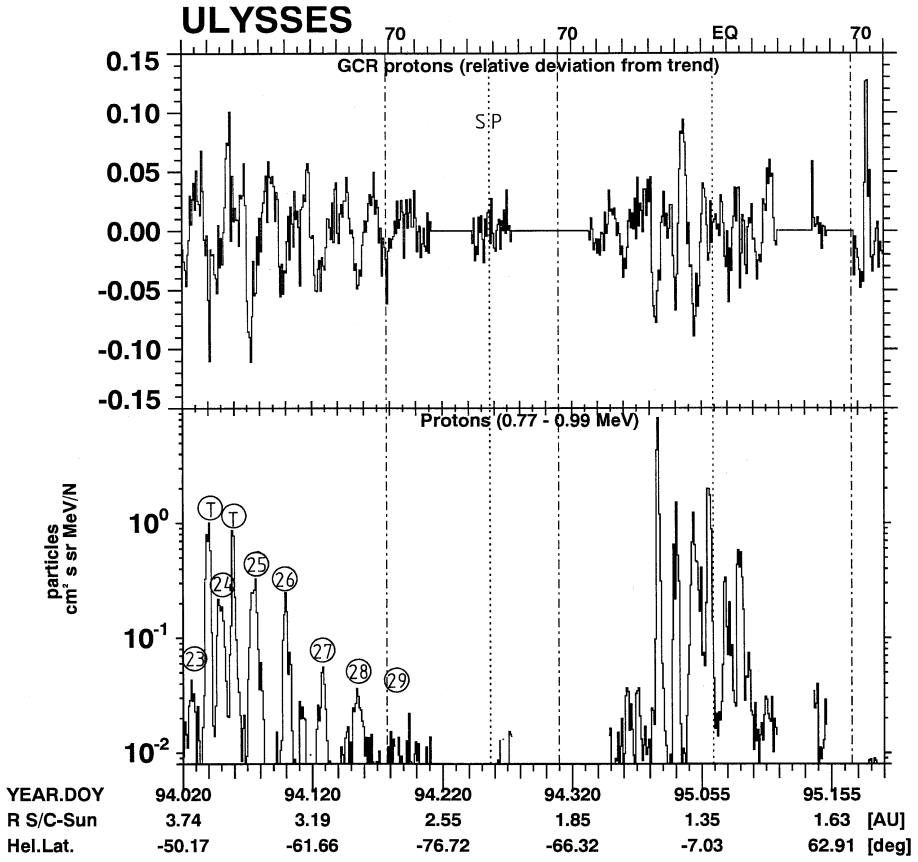

Fig. 5. Detrended counting rates of ELH channels corresponding to protons with energies $E > 230$ MeV along with energetic protons (~ 1 MeV).

in such processes have not been considered in their paper. So acceleration even from solar wind energies on cannot be excluded any longer. The close association of particles and shocks makes it plausible to assume that those particles have actually been accelerated at the shocks.

When ULYSSES passed beyond $-29°$ (following day 120/1993), the ratio between fast and slow solar wind speed dropped from about 2 to 1.4 while the maximum speed remained unchanged. This was the highest latitude to which the solar streamer belt extended (Bame et al. 1993). The latter is thought to surround the heliospheric current sheet (Feldman et al. 1981, Gosling et al. 1981). At higher latitudes the sector structure of the interplanetary magnetic field disappeared and so did the CIR related forward shocks (propagating toward the equator, e.g. Gosling et al. 1993). The reverse shocks were regularly observed up to latitudes of $-42°$ (Gosling et al. 1995). While the CIR existed during the whole period of observation, shocks no longer appeared regularly at ULYSSES. At higher latitudes during the following 6 solar rotations only 3 more R-shocks have been reported by Phillips et al. (1995), the last one at $-58.2°$.

Energetic particles, however, were observed in each solar rotation up to about $-68°$, equally spaced by the $\sim$ 26 day rotation period, which is the equatorial rotation period of solar structures. No evidence for the influence of the differential rotation of the Sun could be found in our data. The conclusion therefore seems to be inevitable that these particles still stem from the CIR related shocks. It would be strange if what had generated the particles while ULYSSES was in lower latitude would no longer generate such particles when ULYSSES had moved to higher latitudes.

In order to discriminate between different mechanisms leading to the observed phenomena, energy dispersion and anisotropies are crucial parameters. During the period when particles were observed along with the shocks, the evolution of the directional distribution needs a more detailed discussion which would fall beyond the scope of this paper. We therefore restrict ourselves here to the more straightforward discussion of those periods where the shocks no longer reached the S/C. In Fig. 4 proton anisotropies for three such events are shown (Compton-Getting correction applied). Despite the large error bars which are enhanced due to the mathematical procedure (spherical harmonic analysis) a weak anisotropy pointing radially inward (i.e. towards the Sun) is observed. The lack of dispersion (Fig. 3) is still maintained in these events. So the model of a temporary magnetic connection to the acceleration region in the distant heliosphere seems to apply more readily (in events like # 9 or 18 this might be even interpreted as occasional and repeated connections). It appears that the particles were accelerated in a continuously operating acceleration process (for example by the CIR related shocks in the distant heliosphere as has been proposed by Simnett & Roelof (1995)). Such a process would also overcome the time constraint for the acceleration process at quasi-perpendicular shocks. So during each solar rotation

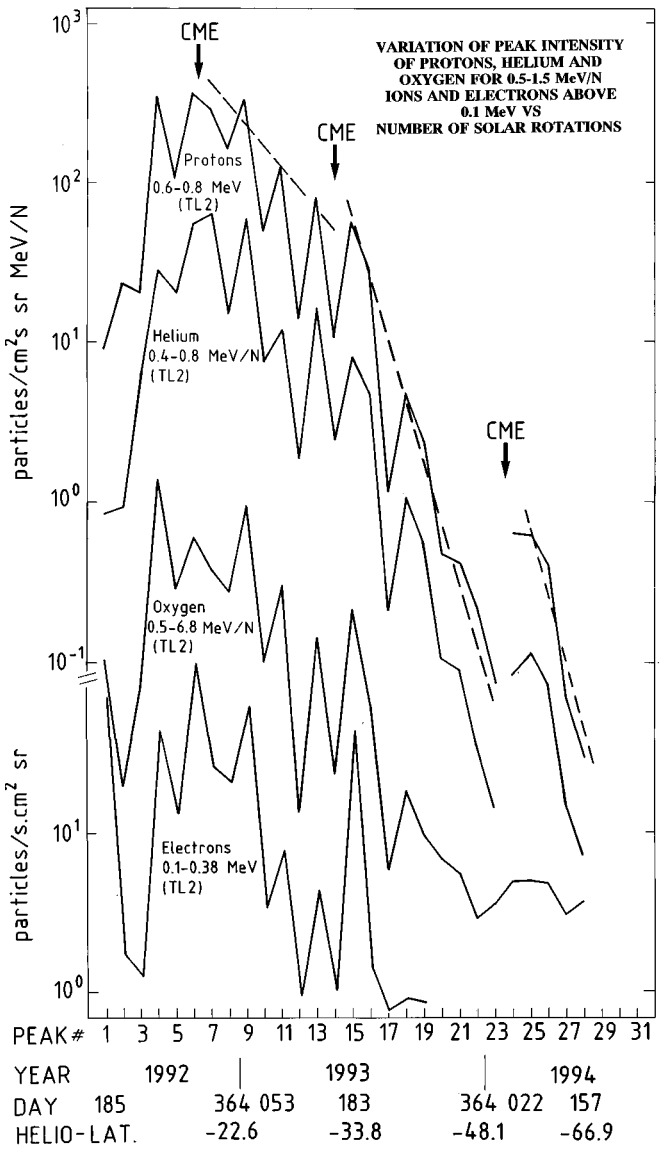

Fig. 6. Variations of observed peak intensities of protons, helium, oxygen and electrons during the high latitude path of ULYSSES. Abscissa is in solar rotations, numbers as in Fig. 1a.

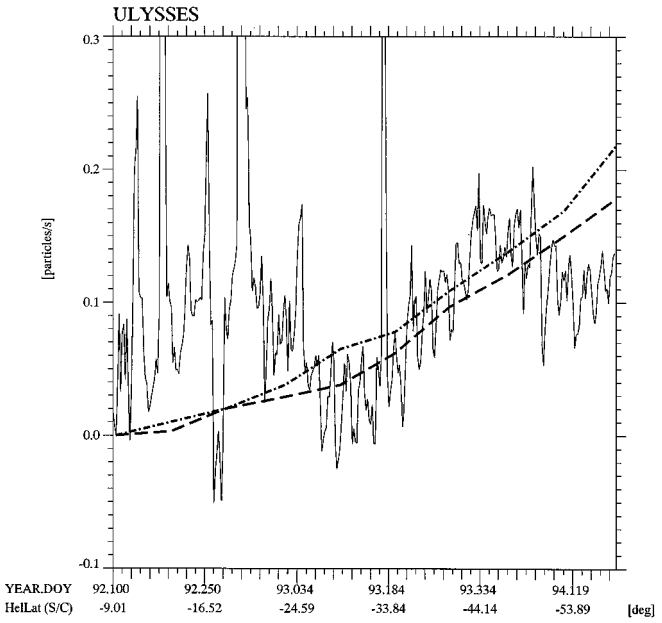

Fig. 7a. Counting rates of the background corrected and normalized ELH channels which are interpreted as being caused by protons with $E > 230$ MeV, from 100/1992 to 185/1994 ($-9°$ to $-55°$ heliographic latitude), together with theoretical expectations (see text for details).

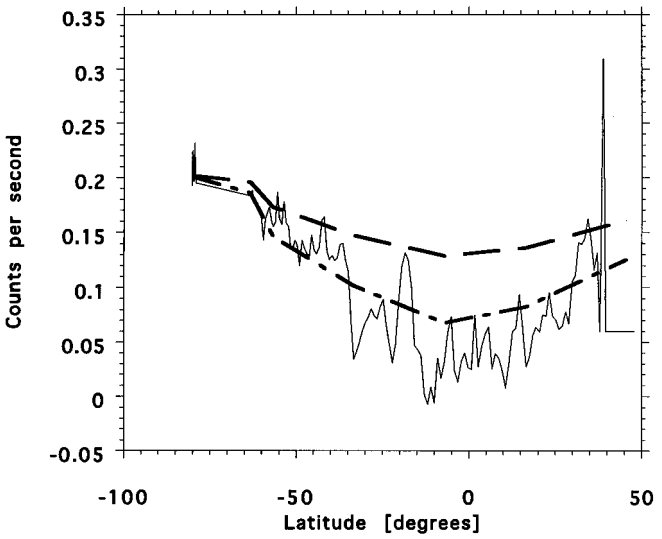

Fig. 7b. Similar to Fig. 7a, for south to north transition pass, $-70°$ to $+70°$ heliographic latitude, again with expected trends from theory (see text for details).

ULYSSES passed through magnetic flux tubes (at high latitudes the field appears to follow approximately an Archimedean spiral bound to conical surfaces (Forsyth 1995, Forsyth et al., 1995)) which connect the S/C to the source region (which could be the shock front). Within such a tube particles of all energies would be observed streaming away from the front. This would result in a dispersion free situation buth with a measurable, weak inward pointing anisotropy in the solar wind frame. This implies that mechanisms had to be sought which would allow energetic charged particles to propagate towards the Sun.

Also the fact, that beyond about $-68°$ energetic particles, i.e., ions with $E > 0.5$ MeV/N (electrons with $E > 100$ keV already beyond about $-30°$) are no longer observed, cannot be easily explained in other models either. If diffusion would actually be the dominant effect, it would be hard to explain why particles did not make it to even higher latitudes. For CIR related events the present findings would reduce the importance of diffusion transverse to the magnetic field as suggested by Kóta & Jokipii (1991) from being a major effect. In the model which we have adopted this implies that connections within magnetic flux tubes no longer exist at higher latitudes above $-68°$. On the other hand reverse shocks associated with CIRs propagate towards higher latitudes (Pizzo 1989 & 1991, Gosling et al. 1993), but weaken as they propagate; they might even barely

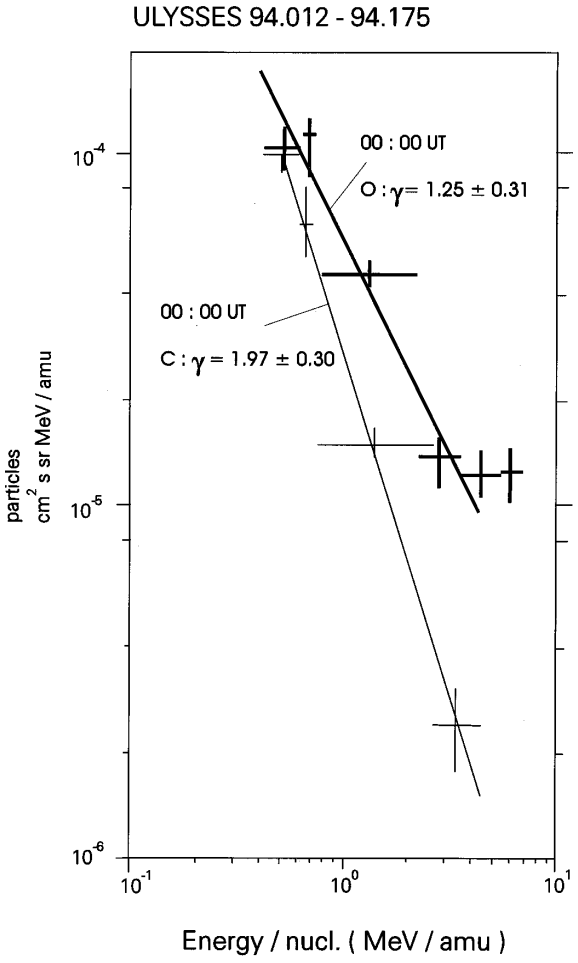

Fig. 8. Energy spectra of C and O during quiet periods in the energy range 0.5 to 6 MeV/N.

propagate beyond about $-55°$ in latitude (Pizzo, private communication, 1996). This agrees nicely with the report by Phillips et al. (1995). We are therefore forced to assume that magnetic flux tubes from higher solar latitudes can meander to lower heliographic latitudes. One mechanism which could be responsible for such a topology could be the turbulence associated with supergranulation on the solar surface; another possibility could be related to the differential rotation of the high latitude photosphere as has been recently pointed out by L. Fisk (preprint 1995). So unlike traditional views, possibilities seem to exist which might be able to establish such connections.

Adiabatic deceleration on the other hand limits the distance which the observed particles could have travelled. It results in energy and momentum loss. The measured energy spectra of the ions had to be considered as being related to a part of the original power law spectrum in kinetic energy at the shock at much higher energies which then has been shifted to lower energies due to the deceleration. If the connection to the shock surface is made at larger and larger distances, the observed spectral range would be related to continuously higher energy bands of the energy spectrum of the energetic particles near the shock. In such an interpretation the observed diminuition in subsequent peak intensities (Fig. 1) of the energetic particles would have been caused by this shift in energy to the associated lower intensity at these higher energies. However, during times where the shocks still reached ULYSSES associated particles with $E > 10$ MeV/N were never seen (R. Marsden, private communication). Also in the more distant heliosphere observed CIR related particle streams never reached such intensities as observed in the present study at energies above about 10 MeV/N (e.g. Van Hollebeke et al. 1978). So we must conclude that the observed accelerated particles stem from such parts of the shocks which are not too far away (a few AU only), so that only minor adiabatic deceleration effects have to be considered. They apparently have propagated within magnetic flux tubes, probably in diffusion-like processes.

The acceleration of particles at collisionless shocks has been reviewed, e.g., by Forman & Webb (1985). To compare theoretical results with observations of energetic particles, it is necessary not only to consider predicted steady state particle distributions, but also time scales for reaching this state. Given the mean free path, it has been shown (Bialk & Dröge 1993, Lim et al. 1996) that the time scales for first order Fermi acceleration are generally too long for the shocks to allow for the required acceleration. We have to leave the question unanswered which mechanism will finally allow to explain the observations. In our view, existing models based on drift and diffusion can not readily explain the observations. For this reason we have also searched for quite different explanations for the observations. In fact, in Quenby et al. (1996b) a different model will be explored. From these discussions we are forced to assume that a consistent theory of the CIR related particle acceleration and propagation is still missing.

We mention in passing another feature of the repetitive energetic particle beams. In Fig. 6 (from Keppler et al. 1995a) we have plotted the maximum intensities of the recurrent beams versus the peak numbers (which is equivalent to time). We note that there is an exponential decay from peak to peak with a time constant of about 35 days. However, after a CME had been observed in situ (indicated in Fig. 1a), the following stream again reached much higher intensities. Subsequent peaks then decayed exponentially as before (Keppler et al. 1995a).

Three such "blow-ups" have been observed; all of them are related to the occurrence of major CMEs. CMEs are known to cause major magnetic disturbances in the inner heliosphere (e.g., Gosling et al. 1981). Due to the decay of the subsequent peak intensities of these corotating flux enhancements we are rather inclined to interpret this behaviour as a function of time: Apparently the CME blows solar material into the heliosphere, so that the shocks find a population of pre-accelerated ions to become accelerated. This population is swept out of the inner heliosphere at time goes by (within 4–5 solar rotations, as shown in Fig. 6) and thus lead to the observed exponential decay in the accelerated peak fluxes. However, after each of the three CMEs mentioned above the decay period starts again but from a smaller peak amplitude as compared to the previous CME;

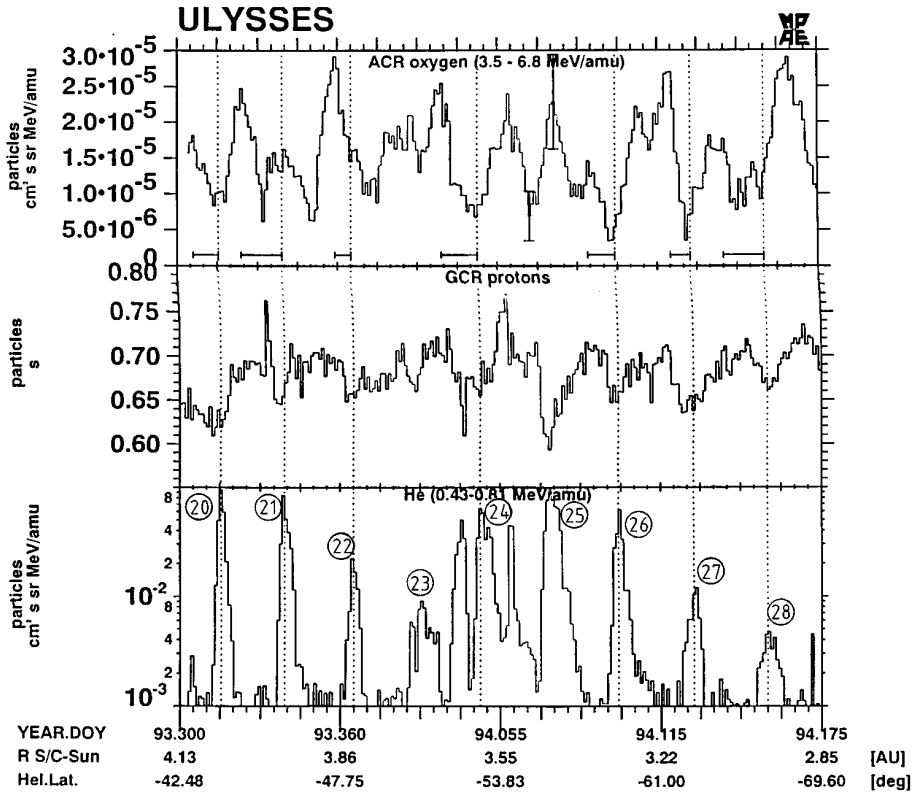

Fig. 9. Fluxes of anomalous oxygen (3.5 to 6.8 MeV/N, upper panel) together with GCR protons ($E > 230$ MeV, mid panel) and helium (0.43 to 0.81 MeV/N, lower panel).

Table 2. Elemental abundances of ions relative to oxygen from EPAC measurements, averaged over forward and reverse shock peaks, respectively, and for quiet periods, together with some published data.

Element	ULYSSES – EPAC			Literature		
	CIR Forward Shocks	CIR Reverse Shocks	Quiet Times[3]	Sol. Min. CIRs[4]	ACR[5]	Fast Solar Wind [6]
p/He[1]	21 ± 4	9.0 ± 3.6	85 ± 40	17 ± 5		21
He[1]	130 ± 30	170 ± 50	263 ± 26	160 ± 50	0.95	45 ± 5
C [1]	0.8 ± 0.1		0.05 ± 0.02	0.89 ± 0.10	0.004	0.529 ± 0.013
Fe[2]	0.11 ± 0.01		0.10 ± 0.05	0.096 ± 0.05		0.124 ± 0.004

[1]For CIRs: Spectral interpolation at 0.7 MeV/amu; errors reflect event-to-event variation
[2]0.6–2.5 MeV/amu; Error of measurement is given
[3]p and He: 0.5–1 MeV/amu; heavier ions: 2.0–6.0 MeV/amu; errors of measurement are given
[4]Richardson et al. 1993
[5]Cummings et al. 1995
[6]Gloeckler & Geiss 1989

this is interpreted as being due to the increased latitude of the subsequent observations.

3. Composition

To determine the relative composition of the particles, we separated the observations into three different types: (I) The accelerated periodic CIR related beams, (II) regularly observed small intensity increases between the beams (interevents), and (III) the quiet periods between the two which will be discussed in Sect. 6. The E-(dE/dx) matrix was used for the composition analysis. This data set has been designed to provide a sample of fully analysed particle events. Because of low count rates in the minima between the periodic events this data set contains all particles that entered the telescope. Coincidences were checked whether they lie in the expected E-(dE/dx) ion tracks. The results are shown in Table 2.

The relative abundances of elements in the CIR related events from July 1992 to June 1994 appear to be consistent with earlier observations in CIRs (see Table 2) (except for the lower p/He ratio), whereas the IEs are characterized by a considerable excess in He and a low fraction of heavy ions. They are also different from the composition of CME related events even though the C/O ratio was consistent with a CME relationship.

4. Galactic cosmic rays (GCR)

4.1. Observations

Below a heliographic latitude of $-14°$, and especially below $-30°$ (after day 50, 1993), the rates (background subtracted as described in Sect. 1) in the "electron channel" ELH of the four telescopes rose continuously (Fig. 7a). In the beginning a few short lasting solar electron events time coincident with electrons of lower energies (shown in Fig. 2) were superimposed on the general trend. These rising fluxes were modulated again with a period of about 26 days, not seen in the ELL channel shown in Fig. 2. Beyond about $-30°$ latitude low energy electrons were observed in only a few transient events. Therefore electrons can be excluded from causing the higher rates. These rates are attributed to high energy protons of the GCR (E>230 MeV), recorded with a geometric factor of 5.3 cm^2sr. Intercalibration with the COSPIN-KET telescope (courtesy H. Kunow) has enabled us to finally confirm the expected response of these chan-

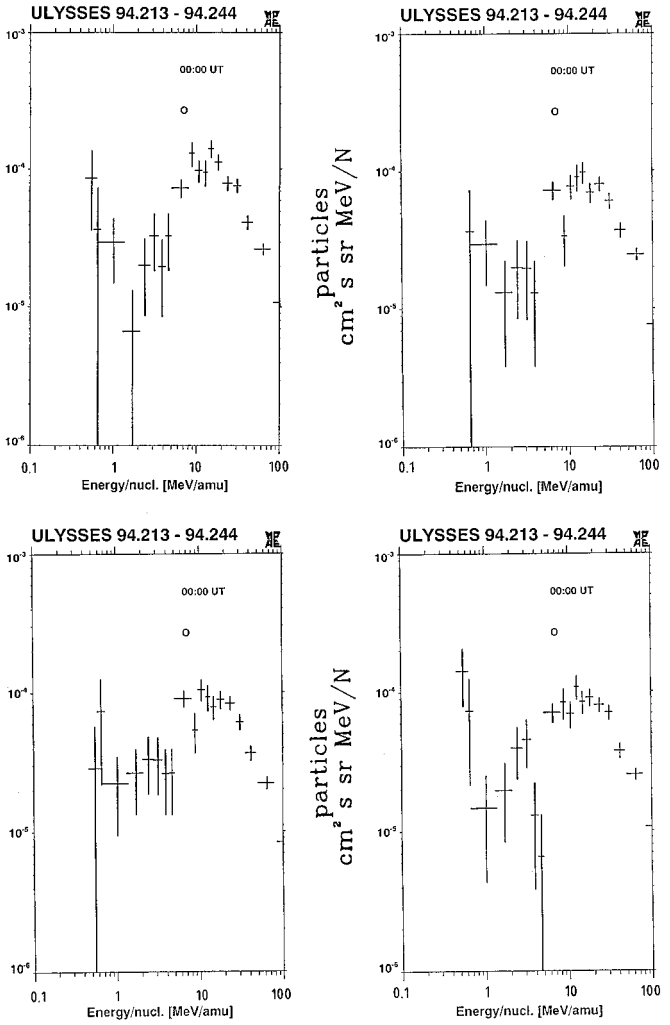

Fig. 10. Energy spectra of anomalous oxygen during quiet periods after switch off of the back detectors, shown for the 4 telescopes T1–T4. This extends the energy range normally covered by the instrument, shown in Fig. 8, to almost 100 MeV/N.

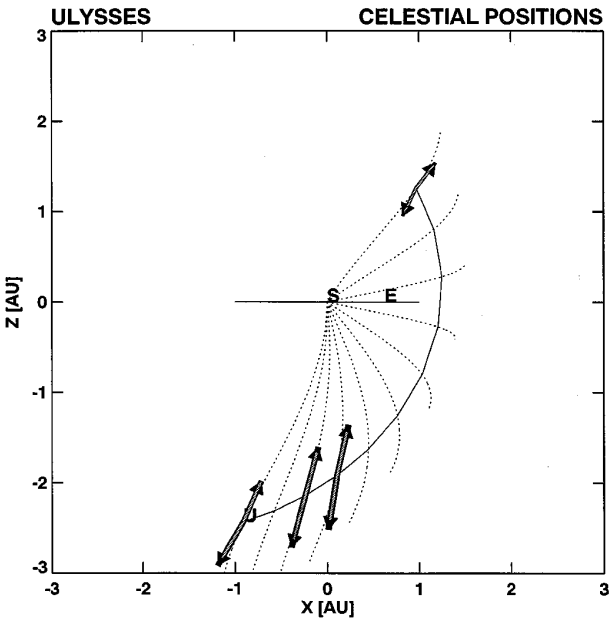

Fig. 11. Total counting rates and anisotropy vectors for anomalous cosmic ray particles measured by the EPAC instrument during the time intervals 213–243/94, 274–304/94, 304–332/94, 131–171/95. The panel shows 30 day averages of the total counting rate as a function of time. The panel shows the projection of the vectors of the first and second intensity maximum of the particle distribution on the ecliptic XY planes. The solid line denoted by "U" is the projection of the ULYSSES orbit on the X-Z plane, the solid line S-E represents the Earth orbit. The relevant time for each vector is its intercept with the ULYSSES orbit line. Thin dashed lines are tangential to the average Parker spiral for a solar wind velocity of 800 km/sec. They start also at the zero line. The hatched part of the vectors represents the isotropic part A_0 of the distribution, the black ends are the residual anisotropies Z_{max}/A_0 in the direction as indicated. Note that the black and grey shaded parts of the vectors represent the ratio of the total intensity in the respective direction to the average intensity. Thus they are NOT a direct representation of the components A_1/A_0 and A_2/A_0, but result from the overlay of both components.

nels and know the absolute cosmic ray rate to better than a factor of two.

4.2. Discussion

The long term rise as well as the 26-day period in the ELH rates are attributed to GCR. The rise shown in Fig. 7a is then interpreted as signature of the recovering GCR flux due to the disappearing solar modulation. This would have been caused partly by time variations and partly by the latitudinal and radial gradients, which have also been observed by others (McKibben et al. 1995, Heber et al. 1995).

The modulated ELH rates and the energetic ion fluxes ($E \sim 1$ MeV/N) were anticorrelated: Maxima in the ELH channels occurred during minima in the ion channels and vice versa, except during three transient events, associated with CMEs, following days 170/1993, 335/1993 and 17/1994 (Fig. 1b, Fig. 8). In Fig. 8, upper panel, the detrended ELH rates are shown representing GCR on an expanded time scale, together with the low energy CIR related He-particles (lower panel). This has also been observed, e.g., by Kunow et al. (1995). Drolias et al. (1995) found an anisotropy and modulation in the GCR from these data, but could not differentiate between inward and outward directions. They found peak fluxes oriented normal to the ecliptic plane. Their findings are very similar to what will be discussed for the ACR below.

5. Gradients of the GCR

To correct the high energy proton fluxes in the background corrected ELH channels (see Sect. 1) for time variations seen near Earth, we use comparable SAMPEX and IMP-8 high energy data and derive for the period 134/1993 to mid 1995 an average flux increase of 11%/year. We assume that the particles observed by EPAC (the average rigidity would be around 1 GV) also follow that increase. The fast passes shown in Fig. 5 were

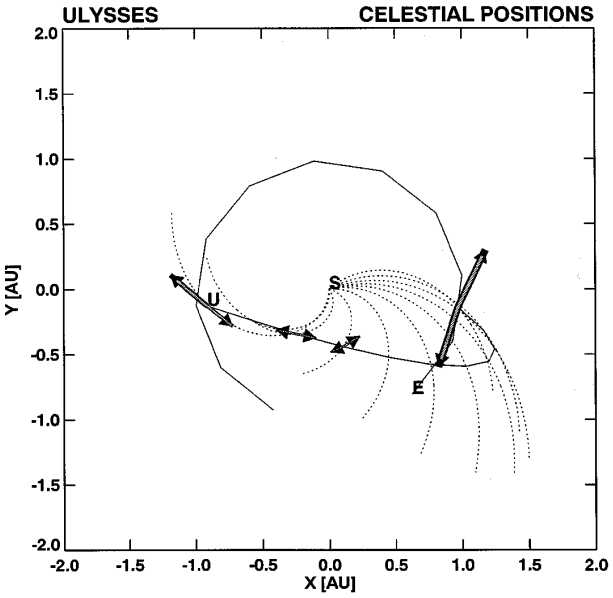

Fig. 12. The trajectory of ULYSSES ("U") projected on the Sun centered ecliptic XY-plane (Earth orbit and position of Earth ("E") shown) for the periods, where these measurements have been made (during 200/1994–195/1995), and the respective ACR flux vector projections as in Fig. 11. The thin grey lines denote the projection of the average Parker spiral for a solar wind velocity of 800 km/sec. See also legend to Fig. 11.

used from $-80°$ through the equator to $+80°$ to determine, after correction for the time related increase of the intensity, the latitudinal gradient (LG) in a first approximation. For the period 129/1994 to 256/1994, a radial gradient (RG) of -3%/AU was derived after correction with the preliminary LG. Then the LG was corrected for the RG and finally for both periods +0.3 to +0.4%/degree was obtained. Similar to the GCR, the LG of the ACR has been shown to be positive in this solar cycle (Cummings et al. 1995), but has changed sign in previous subsequent cycles. Both have positive charges, thus these findings underline the importance of drifts for the propagation of high energy particles in the heliosphere.

In a previous paper (Quenby et al. 1996a) we discussed the relativistic cosmic ray latitude effect, as seen by EPAC on the first, 1993–1994 pass over the south polar regions. Further inspection of Fig. 7 shows that the rise in the observed intensity of the GCR was interrupted between 334/1993 and 129/1994 and between 256/1994 and 330/1994. During both intervals the solar activity was very low, so it is unlikely that this break in the recovery of GCR has been directly caused by solar activity. Fig. 7a, adapted from Quenby et al. (1995) shows the RTG and SAMPEX corrected relativistic proton rate (averaged over 2.5 days) from EPAC, plotted against latitude. We have repeated this work for the first south-north pass in Fig. 7b. Normalisation was made for the southern pass (Fig. 7a) at $-9°$ and for the transition from south to north (Fig. 7b) at $-80°$. Superimposed two theoretical curves are shown, taken from Potgieter & Haasbroek (1993) which includes full drift modulation (dashed curve), while the dot-dashed curve represents the Jokipii & Kóta (1989) modified drift theory as interpreted by Potgieter (private communication), the predictions are for 1.2 GeV protons. The plots refer to particles in excess of those recorded on day 100, 1992.

The conclusion of this previous work (Quenby et al., 1996a) was that although the full drift theory was not inconsistent with the magnitude of the latitude effect, a very significant latitude dependent wave appears in the plot (Figs. 7). It was suggested that local, latitude dependent control of modulation was occurring with the effects of the activity belt at $15° - 30°$ south most prominent. A modulation model with mainly radial diffusion and much reduced drift would appear to be necessary to reproduce such features. In order to check the previous result with subsequent polar pass data, we see in Fig. 7b (corrected EPAC data taken on the south-north pole passage) a magnitude of the latitude effect similar to that of Fig. 7a, and an indication of a wave in the counts versus latitude curve again apparent in the south polar to equator leg of the data with minimum at about $30°$ south. To the north of the equator, the data is more sparse, due to mode switching of the instrument, and no conclusions may be drawn concerning the persistence of the wave. Thus these more recent data lend some extra, but not overwhelming support to the previous suggestion that local, latitude dependent modulation control is dominant at small solar distances.

6. Anomalous Cosmic Rays (ACR)

6.1. Observations

In the quiet periods between the recurrent events the energetic particle fluxes were low, but not zero. In order to identify the composition of the underlying population, we had to integrate over longer time intervals in order to obtain statistically significant informations. We therefore made the assumption that even over times of the order of several months the population of interest did not change its character (which we cannot prove, however, assume to be reasonable). In order to eliminate periods where the (typically larger) fluxes of CIR related particles were present, a threshold to the observed rates was set in a He-channel at a rate of 0.03 ions $(\mathrm{cm}^2\ \mathrm{sr\ s\ MeV/N})^{-1}$. Then rates were accumulated during periods where the intensity of that channel fell below this threshold (Blake et al. 1995).

These quiet periods are characterized by low C/O ratios (only slightly higher than known for ACR, cf. Table 2), which suggests the presence of the ACR probably together with particles of other origin, which is likely in view of the energy range (2–6 MeV/N) where the data have been taken. Typical quiet time energy spectra of carbon and oxygen in the energy range 0.4 to 5 MeV/N are shown in Fig. 9. The oxygen spectrum which for its lower energy portion can be described by a power law in energy with an exponent of -1.25 shows an upturn above 3 MeV/N, while the carbon spectrum remains at a power law with an exponent of about -2 which is consistent with particles of solar origin. The upturn in oxygen, however, indicates the presence of ACR (which we already suggested from the C/O

ratio) probably together with particles of other origin (Keppler et al. 1995b, Fraenz et al. 1995a). The C/O ratio in the energy range 2 to 6 MeV/N was C/O = 0.05±0.02, a value which is similar to that observed for the ACR near Earth (Cummings & Stone 1990, Adams et al. 1991). We have not found variations of the observed level in the quiet time fluxes related to the movevent of ULYSSES in heliographic latitude.

Analysis of spectra and composition revealed that the anomalous component made up a substantial contribution to the observed oxygen fluxes in the "quiet times" between the recurrent flux increases during 1992 and 1993 (cf. Blake et al. 1995). From the measured spectra and the observed abundance ratio of C/O we conclude that the quiet time fluxes which underlie all observations are due to particles belonging to the anomalous component of cosmic rays. It is therefore justified to say that this component is present throughout the inner heliosphere at all latitudes.

Due to solar-cycle modulation and latitudinal gradients, the ACR fluxes rose with time, whereas the peak intensities of the CIR induced increases decreased after the corotating shocks were no longer observed in situ. This had the consequence that beyond -42° latitude fluxes of CIR accelerated oxygen above 3.5 MeV/N did not surpass the ACR level. This made it possible to study time variations of the ACR, with disturbances only from transient events. We observed a recurrent variation with the (low latitude) solar rotation period, which is correlated with the flux of GCR and anticorrelated with the flux of CIR accelerated particles. Fig. 9 shows GCR protons (from our ELH channels) and ACR oxygen (3.5–6.8 MeV/N) together with low energy helium fluxes (0.43–0.81 MeV/N, lower panel). The amplitude of this variation turned out to be much larger than that observed for the GCR (Reuss et al. 1996). This observation is consistent with previous reports of 26 day variations of ACR observed from the Pioneers and Voyagers between 1 and 14 AU in the two previous solar cycles (Garcia-Munoz et al. 1977, Bastian et al. 1979, Webber et al. 1979, von Rosenvinge & Paizis 1981, Cummings & Webber 1983). This variation could be observed on the southbound pass from -42° up to the last observed recurrent increase in accelerated particles of lower energy and again on the pole to pole passage from -36° to $+30^\circ$.

This kind of modulation is also observed in ground based neutron monitor data (Simpson et al. 1995), so it must be inferred that the underlying mechanism affects GCR and ACR up to the highest rigidities. We emphasize that this modulation region must rotate with the Sun's rotation rate and must be finite in its longitudinal extension; otherwise the 26 day modulation could not be understood. It is obvious that the minima of the high energy fluxes coincide with the maxima of the low energy particles. The latter have been numbered according to the scheme adopted in Fig. 1. They are in our view particles accelerated at the CIR related shocks (as already mentioned, only 3 R-shocks passed at ULYSSES during this period). The shocks seem to influence the propagation of the high energy cosmic rays as well as the ACR which is of much lower energies, however, as it is mainly singly charged of comparable rigidity. This demonstrates quite clearly that the variation in the high energy fluxes must be related to the passage of the CIR through a region from where magnetic flux tubes could guide the low energy particles back to ULYSSES. This conclusions are also in general agreement with what has been stated in Sect. 2.

The CIR might then be viewed as kind of a "shield" which reduced the flux of the particles from a certain range of directions; it would have limited extension, and rotate with the Sun. The apparent modulation depth could in such a model reflect the solid angle under which this region is seen from our detectors. Once the CIR has moved to the opposite (more distant) side of the Sun, it would appear under a smaller solid angle so that the particles – assumed to show isotropic angular distribution – can arrive from a larger fraction of the sphere at the detectors. The effect may be understood in terms of the increased turbulence between the two shocks which can reduce the diffusion length. Such conclusions have been also drawn earlier, e.g., by Zangh & Burlaga (1988).

In order to extend the energy range of the EPAC instrument to higher energies, the veto-detectors were switched off for several weeks (this was done during four periods: 214/1994 to 244/1994, 287/1994 to 326/1994, 121/1995 to 140/1994, 152/1995 to 171/1995 when ULYSSES was in high south and north heliographic latitudes). In this mode ions that penetrate the E-detector form a "return trace" in the E-(dE/dx) matrix. However, each point on this track may be contributed to by different heavy ion species of different energies. The measurements are obtained by accumulating ACR oxygen, neon and nitrogen particles in the energy range 5–25 MeV/N (1.5–3.5 GV rigidity) and subtracting the high energy cosmic ray background (mainly iron, $E > 500$ MeV/N) of 10% which we assumed to be isotropic. By carefully correcting for the energy losses of heavier ions, the spectrum of anomalous oxygen could be extended up to 100 MeV/N (Fraenz et al. 1995a). This procedure yielded an oxygen spectrum for each viewing direction of the instrument (Fig. 10). Probably due to the difficult corrections in calculating the contributions of the heavier ions to the various energy channels in the thus degraded instrument the peak of the spectrum appears to be higher by about 20% compared to measurements of the COSPIN-LET instrument on ULYSSES (K.J. Trattner, personal communication). But the shape of the spectrum for the underlying component became clearly visible and is shown in Fig. 10.

Fraenz et al. (1995b) and Drolias et al. (1995) have derived anisotropies for both the ACR and the GCR. We take advantage of the full 4π coverage due to the 4 telescopes and 4 sectors per spin revolution. The measured distributions are interpolated and analyzed by spherical harmonic analysis. In order to investigate the anisotropy of the ACR, higher count rates for ACR oxygen were needed. For this reason only periods have been used for this analysis where the backdetectors in all four telescopes had been switched off, because this gave much higher rates. For the anisotropy calculation the rates from the four telescopes have been corrected in the same way. The conclusions derived from these data are based on their relative differences and will therefore not be changed even by the presence of a residual "background". A detailed discussion on procedure and results will be

Table 3. EPAC C-off Anisotropies

No.	1	2	3	4
Period	213–243/94	274–304/94	304-332/94	131–171/95
Counts	790	710	508	800
$\sqrt{2/c}$	5	5	6	5
$\sqrt{3/c}$	6	6	8	6
$\sqrt{1/c}$	4	4	4	4
A_0	6.0	5.4	4.0	4.1
A_1/A_0	9	5	6	7
A_2/A_0	14	19	27	15
s_θ	0.5	1.0	1.0	0.7

This table contains the anisotropy parameters for 12 time intervalls where the C-detector had been switched off.
The parameters are:

Counts: Total counts collected along oxygen track between 5–25 MeV/N after subtraction of foreign contributions.

$\sqrt{2/c}$: Expected statistical anisotropy [%] by error propagation.

$\sqrt{3/c}$: Expected statistical anisotropy [%] by simulation (Zwickl & Webber 1976), if applicable to three dimensions.

$\sqrt{1/c}$: Standard deviation of these anisotropies.

A_0: Isotropic intensity [10^{-5} particles/(s cm^2 sr MeV/N]

A_1/A_0: first order anisotropy [%]

A_2/A_0: second order anisotropy [%]

s_θ: Stand.dev. for first order angle [rad]

The spatial resolution corresponding to 4 polar and 4 azimuthal sectors (spatial angle = $\pi/4$) is assumed to result in a standard deviation of $\pm\pi/4$ for the anisotropy direction.
The isotropic intensity is not a linear function of the total counts since the actual measuring time differs from period to period.

published elsewhere (Fraenz et al. 1996). Several attempts have been made to determine the density distribution of the ACR by a comparison of the bulk flux density of anomalous oxygen at different locations in the heliosphere (Cummings et al. 1995; Trattner et al. 1995). The LG of the ACR for the current solar polarity has been reported to be 2%/degree, in agreement with models.

Figs. 10 and 11 show the two main flux vectors of the ACR particle distribution from 30 day averages during the four intervals (213–243/94, 274–304/94, 304–332/94, 131–171/95) located at the position of the ULYSSES spacecraft in interplanetary space at the time of measurement. The vectors are projected on the XZ and XY planes of the ecliptic system. The thin grey lines given for 30 day intervals denote the direction tangential to the average Parker spiral for a fixed solar wind velocity of 800 km/sec. The light hatched parts of the flux vectors denote the unit sphere, corresponding to the isotropic part A_0 of the particle distribution. Thus the black part of each vector corresponds to the actual anisotropic part Z_{max}/A_0, where Z_{max} is the absolute maximum of each distribution. This value reaches a maximum of 1.27 for the interval 304–332/94.

Note that in Fig. 11 the axis extends to 6 AU but in Fig. 12 to 4 AU only. The inclination of the current sheet and of the solar magnetic equator (7°) have been neglected. Anisotropies with an acceptable uncertainty have been derived from sums over all oxygen counts in the energy range 5.0–25.0 MeV/amu, i.e. sums over the whole anomalous peak of the spectrum. The underlying numbers are given in Table 3 show that the first order anisotropy never exceeds the statistical value of $6 \pm 4\%$.

We see from Table 3 and the figures: (1) The particle distributions for the south polar passage are more or less field aligned while for the north polar passage the orientation is in general normal to the field. (2) All distributions have a large bidirectional component since there are typically two intensity maxima nearly opposite to each other.

For a solar wind velocity of v = 800 km/sec the convective anisotropy $A = 2(\gamma + 1)v/V$, where v denotes the particle speed, V the solar wind speed and γ the exponent of a power law spectrum in energy per nucleon, for 10 MeV/N particles is approximately 5% because γ is very small. This anisotropy is negligible in comparison to the bidirectional anisotropies of 14-27%. The modulation of galactic cosmic rays by corotating interaction regions at high solar latitudes has been observed by several authors (e.g., Keppler et al. 1995b, Quenby et al. 1995, Simpson et al. 1995). The anomalous component of cosmic rays is obviously modulated in the same way (Reuss et al. 1996). The main point here is that ACR drifts caused by this modulation are much stronger than any other measurable drift at solar distances larger than 1.5 AU. The observed anisotropy pattern suggests that within the region of modulation ACR particles stream field aligned with a large bidirectional component within the undisturbed fields before and behind the corotating global CIR structure.

For the north polar pass the situation is apparently different from that found during the southern pass. Here the anisotropy is apparently more or less normal to the field but again directed away from the Sun. This might be due to the smaller distance from the Sun compared to the southern pass. This finding concurs with the model which has been put forward by Quenby et al. (1995), where the intensity maxima (for protons) have been predicted to be normal to the average field. We infer from this that current models for cosmic ray drifts in the heliosphere cannot be applied for regions closer to the Sun than about 1.8 AU (from Fig. 11) where other features seem to have dominated the CIR modulation which caused the observed pattern in the southern hemisphere at somewhat larger distances (1.5–2.7 AU). A more comprehensive account to this topic will be given in a forthcoming paper.

7. Summary

We discussed the acceleration of energetic ions and electrons in CIR related shocks and concluded that, for the case where the shocks could no longer be observed at ULYSSES, these particles may have been accelerated at shocks in the more distant heliosphere and have been guided to ULYSSES in magnetic flux tubes which temporarily connected the observer with the distant acceleration region. This conclusion was based (i) on the lack of energy dispersion of the particles and (ii) on the inward directed anisotropy. We cannot resolve whether such flux tubes have been bent equatorwards towards the shocks still at lower latitudes or whether the connection led to shock fronts which had moved

to higher heliographic latitudes in the distant heliosphere (say beyond 10 AU or so).

Composition measurements have revealed that underlying the observed energetic particle streams there are anomalous cosmic rays and the galactic cosmic rays recovering from solar cycle modulation. Both are modulated by a 26-days period through all latitudes, i.e. the low latitude solar structures determine the behaviour of these particles. The modulation is anticorrelated to the energetic particle streams which are associated with the CIRs. For this reason we tentatively argue that this modulation is caused by scattering of the particles in the enhanced turbulence associated with the CIR resulting in kind of "shadowing" effect. Anisotropies for the GCR are normal to the ecliptic plane (but we could not distinguish up or down), for the ACR radially outward during the southern hemisphere pass during a period where the distance to the Sun was somewhat larger than during the period when the measurements in the northern hemisphere were performed. In the northern hemisphere the anisotropy was in general normal to the average magnetic field but also pointing away from the Sun.

Acknowledgements. We have used the solar wind velocity derived from the SWICS instrument, courtesy G. Gloeckler, and magnetic field data from the ULYSSES magnetometer, courtesy A. Balogh. We thank J. Woch for providing to us the solar wind data and stimulating discussions. We are grateful for the help in preparing the data to S. Mazuk and M. Bruns. The support of the project scientists and the staffs of the ULYSSES Project Offices at JPL, ESTEC, and ESOC is gratefully acknowledged. This work was supported by the Max-Planck-Gesellschaft zur Förderung der Wissenschaften e.V. and by DARA under grant no. 50 ON 91050.

We appreciate valuable comments and suggestions by F.B. McDonald in evaluating this paper.

References

Adams J.H., Garcia-Munoz M., Grigorov N.L. et al., 1991, Proc. 22nd ICRC, Dublin, 3, 358.

Bastian T.S. McKibben R.B., Simpson J.A., 1979, Proc. of the 16th ICRC 12, 324.

Balogh A, Erdös G, Forsyth R.J., Smith E.J., 1993, GRL 20, 2331.

Balogh A., Gonzalez-Esparza J.A., Forsyth R.J. et al., 1995, Space Sci. Rev. 72, 171.

Bame S.J., Goldstein B.E., Gosling J.T. et al., 1993, GRL 20, 2323.

Barnes C.W., Simpson J.A., 1976, ApJ 210, L91.

Bialk M., Dröge W., 1992, Proc. 23rd ICRC, Calgary, 3, 278.

Blake J.B., Fraenz M., Keppler E. et al., 1995, Adv. Space Res. 15, (7)81.

Cummings A.C., Stone E.C., 1990, Proc. 21st ICRC, Moscow, Vol. SH, 202.

Cummings A.C., Webber W.R., 1983, Solar Wind 5, NASA-CP 2280, p. 427.

Cummings A.C., Mewaldt R.A., Blake J.B., Cummings J.R. Fraenz M., Hovestadt D., Klecker B., Mason G.M., Mazur J.E., Stone E.C., von Rosenvinge T.T., Webber W.R., 1995, GRL 22, 341.

Drolias B., Quenby J.J., Reuss M.K., Blake J.B., Fraenz M., Keppler E., Witcombe A., 1995, Proc. 24th ICRC, Rome, Vol. 4, 976.

Feldman W.C., Asbridge J., Bame S.J., Fenimore E.E., Gosling J.T., 1981, J. Geophys. Res. 86, 5408.

Forman M., Webb G.M., 1985, in Collisionless shocks in the heliosphere, AGU Monographs, Vol. 34, 91.

Forsyth R.J., 1995, Space Sci. Rev. 72, 153.

Forsyth R.J., Balogh A., Smith E.J., Murphy N., McComas D.J., 1995, GRL 22, 3321.

Fraenz M., Keppler E., Krupp N., Reuss M.K., Blake J.B., 1995a, Space Sci. Rev. 72, 339.

Fraenz M., Blake B., Drolias B. Keppler E., Quenby J.J., Reuss M.K., Seidel R., Witcombe A., 1995b, Proc. 24th ICRC, Rome, Vol. 4, 820.

Fraenz M., Blake J.B., Keppler E., Reuss M.K., 1996, to be published.

Garcia-Munoz G., Mason M., Simpson J.A., 1977, Proc. of the 15th ICRC, 3, 209.

Gloeckler G., Geiss J., 1989, AIP Conf. Proc., 183, 49.

Gloeckler G., Geiss J., Roelof E.C., Fisk L.A., Ipavich F.M., Ogilvie K.W., Lanzerotti L.J., von Steiger R., Wilken B., 1994, J. Geophys. Res. 99, 17637.

Gosling J.T., Borrini G., Asbridge J.R., Bame S.J., Feldman W.C., Hansen R.T., 1981, J. Geophys. Res. 86, 5438.

Gosling J.T., Bame S.J., McComas D.J., Phillips J.L., Pizzo V.J., Goldstein B.E., Neugebauer M., 1993, GRL 20, 2789.

Gosling J.T., Bame S.J., McComas D.J., Phillips J.L., Pizzo V.J., Goldstein B.E., Neugebauer M., 1995, Space Sci. Rev. 72, 99.

Heber D., Raviart A, Paizis C. et al., 1995, Space Sci. Rev. 72, 391

Hoeksema J.T., 1995, Space Sci. Rev. 72, 137.

Hundhausen A.J, Gosling J.T., 1976, J. Geophys. Res. 81, 1436.

Jokipii J.R., Kóta J., 1989, GRL 16, 1.

Keppler E., Blake J.B., Hovestadt D., Korth A., Quenby J.J., Umlauft G., Woch J., 1992, A&AS 92, 317.

Keppler E., Fraenz M., Krupp N., Reuss M.K., 1995a, Nuclear Physics B (Proc. Suppl.) 39A, 87.

Keppler E., Fraenz M., Korth A., Reuss M.K., Quenby J.J., Blake J.B., Witte M., 1995b, Science 268, 1013.

Kóta J., Jokipii J.R., 1991, GRL 18, 1797.

Kunow H., Dröge W., Heber B., Müller-Mellin, Röhrs K., Sierks H., Wibberenz G., Ducros R., Fernando P., Rastoin C., Raviart A., Paizis C., 1995, Space Sci. Rev. 72, 397.

Lim T.L., Quenby J.J., Reuss M.K., Keppler E., Fraenz M., 1996, Ann. Geophys., in press.

McKibben R.B., Connell J.J., Lpate C., Simpson J.A., Zhang M., 1995, Space Sci. Rev. 72, 367.

Phillips J.L., Bame S.J., Barnes A., Barraclough B.L., Feldman W.C., Goldstein B.E., Gosling J.T., Hoogeveen G.W., McComas D.J., Neugebauer M., Suess S.T., 1995, GRL 22, 3301.

Pizzo V.J., 1991, J. Geophys. Res., 96, 5405.

Pizzo V.J., 1994, J. Geophys. Res., 99, 4173.

Pizzo V.J., Gosling J.T., 1994, GRL 21, 2063.

Potgieter M.S., Haasbroek L.J., 1993, Proc. of the 23rd ICRC, 3, 457.

Quenby J.J., Drolias B., Keppler E., Reuss M.K., Blake J.B., 1995, GRL 22, 3345.

Quenby J.J., Drolias B., Keppler E., Reuss M.K., Blake B.J., 1996a, Solar Phys. 163, 397.

Quenby J.J., Witcombe A., Drolias B., Fraenz M., Keppler E., 1996b, A&A, this issue.

Reuss M.K., Fraenz M., Keppler E., 1996, Ann. Geophys., accepted for publication, 1996.

Richardson I.G., Barbier L.M., Reames D.V., von Rosenvinge T.T., 1993, J. Geophys. Res. 98, 13.

Roelof E.C., Simnett G.M., Armstrong T.P., 1994, Space Sci. Rev. 72, 309.

Simnett G.M., Sayle K.A., Roelof E.C., 1995a, GRL 22, 3365.

Simnett G.M., Roelof E.C., 1995b, Space Sci. Rev. 72, 303.
Simpson J.A. et al., 1995, Science 268, 1019.
Smith E.J., Wolfe J.H., 1976, GRL 3, 137.
Smith E.J. et al., 1993, GRL 20, 2327.
Trattner K.J. et al., 1995, GRL 22, 3349.
Van Hollebeke M. et al, 1978, J. Geophys. Res. 83, 4723.
Von Rosenvinge T.T, Paizis C., 1981, Proc. of the 17th ICRC 10, 69.
Webber W.R., Stone E.C., Vogt R.E., 1979, Proc. of the 16th ICRC 5, 357.
Zhang G., Burlaga L.F., 1988, J. Geophys. Res. 93, 2511.
Zwickl R.D., Webber W.R., 1976, NIM, 138, 191.